

Novel geothermal gradient map of the Croatian part of the Pannonian Basin System based on data interpretation from 154 deep exploration wells

M. Macenić, T. Kurevija^{*}, I. Medved

Faculty of Mining, Geology and Petroleum Engineering, University of Zagreb, 10000, Croatia



ARTICLE INFO

Keywords:

Geothermal gradient
Bottomhole mud temperature
Virgin rock temperature
Geothermal map
Drillstem test
Renewable energy source

ABSTRACT

As part of EU strategy to tackle climate changes, energy transition from fossil fuels to renewable resources is necessary. During the last few years, in the Republic of Croatia there is a strong tailwind towards promoting activities of geothermal energy exploration and exploitation. As geothermal sector was often neglected in a favour of petroleum business in the past, there is still a somewhat knowledge gap in groundwork related to defining geothermal resources potential. Since initial investigation related to defining hot spots in geothermal gradient were conducted more than 40 years ago, there was a need to remodel older imprecise maps with a completely new groundwork research in this area. More than 150 deep oil&gas exploration wells scattered in the Croatian part of the Pannonian Basin were elaborated. From the historical well development records and temperature measurements, obtained with different methods, a novel geothermal gradient map was constructed. Furthermore, to define local potential sites for direct heat utilization and electricity production, temperature maps were designed for a depth of 1000 and 2000 m, respectively.

1. Introduction

The use of geothermal potential is recognized and recommended in strategic plans and programmes in European Union (EU). After the process of updating energy goals at the end of the 2016, European Commission has published new energy legislative framework – the Clean Energy for All Europeans package. These new rules were formally adopted at the beginning of 2019 and they consist of eight different legislative acts. Most important binding target of a new framework is reaching at least 32% of renewable energy share and achieving energy efficiency target of 32,5% until 2030. Also, during December of 2019, European Green Deal was introduced to make EU climate-neutral continent by setting new growth strategy and to decarbonise energy sector based on renewable energy resources, including geothermal energy. In the new Renewable Energy Directive (EC 2018/2001) [1], deep and shallow geothermal energy were both recognized as an important local renewable energy source which should be exploited wherever possible. To achieve binding targets, each Member State must carry out an assessment of their potential of energy from renewable sources.

In the Republic of Croatia, geothermal energy exploration and prominent sites discoveries were always historically linked closely to petroleum sector activities. Exploration and exploitation of

hydrocarbons resources in Croatia has resulted in the drilling of more than 4000 deep wells over the last 70 years [2]. Alongside discoveries of oil and gas reserves, significant number of geothermal brine reservoirs and hydrocarbon bottom aquifers have been identified, with prospective flow and thermodynamic properties for long-term exploitation of renewable energy. Currently, majority of the hydrocarbon reservoirs in Croatia are in the final phase of exploitation with a continuous decline in production. While petroleum sector is still of strategic importance to the economy, the question of the oil upstream industry future is being raised in a long-term. Therefore, according to new EU energy framework, there is a need of partial transition from oil business to geothermal energy, since technology and infrastructure are almost similar in nature. The main barrier to the widespread development of geothermal energy sector in Croatia lies in the intensive capital investment, a higher risk factor for the investor in exploration phase, and a still incomplete regulatory and financial-economic framework for exploiting such resources. Borović and Marković [3] gave comprehensive study when it comes to utilization of low enthalpy geothermal brines in Croatia, usually used in recreational and balneology purposes in numerous spas and recreation centres, with emphasis on still untapped and unused geothermal potential. When it comes to utilizing available geothermal sources for direct heating purposes only small potential is used for heating mostly greenhouses and only few buildings [3]. However,

* Corresponding author.

E-mail address: tkurevi@rgn.hr (T. Kurevija).

Nomenclature		Subscripts/superscripts
Symbols		BH bottomhole
D	depth, m	c circulation time
d_{ij}	distance between points i and j	f formation
g	geothermal gradient, °C/m	s surface
h	fixed distance, lag	
q'	heat transfer rate, W/m	
t	time, s	
Δt	time since circulation stopped, s	
T	temperature, °C	
λ	thermal conductivity, W/m°C	
Δ	spatial width with a center at h	

Acronyms/abbreviations	
BHT	bottomhole temperature
CPBS	the Croatian part of the Pannonian Basin System
DST	Drill Stem Test
EGS	Enhanced Geothermal Systems
ORC	Organic Rankine Cycle
RMS	root-mean-square
VRT	Virgin Rock Temperature

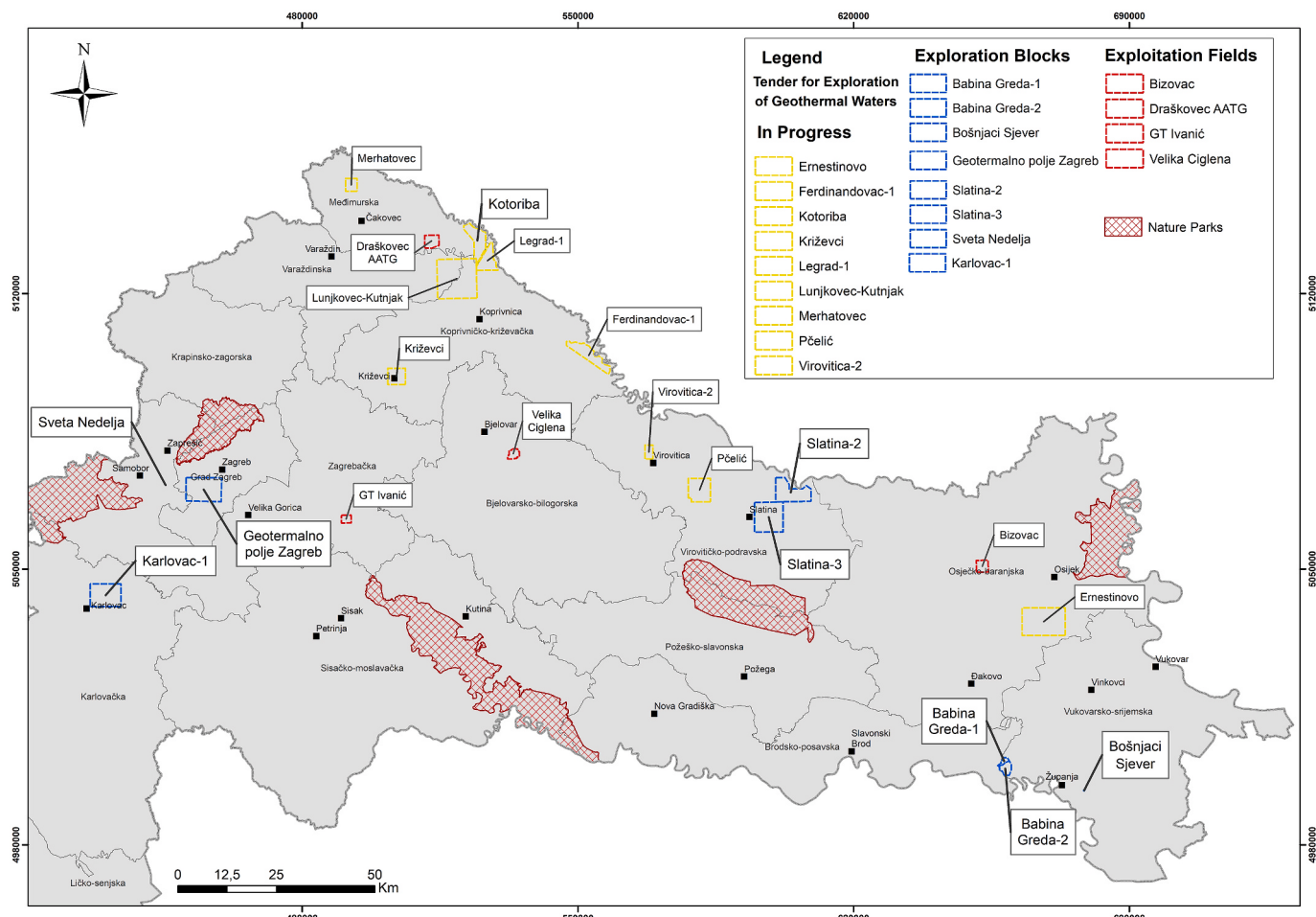


Fig. 1. Current exploitation fields, exploration blocks and publicly announced tenders for exploration of geothermal reservoirs (with permission of Croatian Hydrocarbon Agency).

recently there has been a development in the sector of electricity production with the 17,5 MW ORC geothermal power plant Velika Ciglena, the first one in Croatia.

During the evaluation process of locating geothermal prospective sites, initial step is to investigate available maps of geothermal gradient or heat flow. Jelić [5] did the first research concerning the thermogeological properties of two Pannonian sub-basins; Sava and Drava. The research was done on collected data from 120 wells. The research was later extended to the entire area of the Republic of Croatia [6]. In this

literature details on interpolation method are missing and some of the information on input data used are no longer available. Furthermore, for the continental part of Croatia most of the data was collected before 1979, when mostly there were no DST (Drill Stem Test) performed in the wells. Therefore, due to poor resolution of the maps produced, no clear information on interpolation method used and older digital versions being irretrievable and unfortunately lost, the need for completely new groundwork research was a necessity.

Mapping of geothermal gradient values is recognized as a first step in

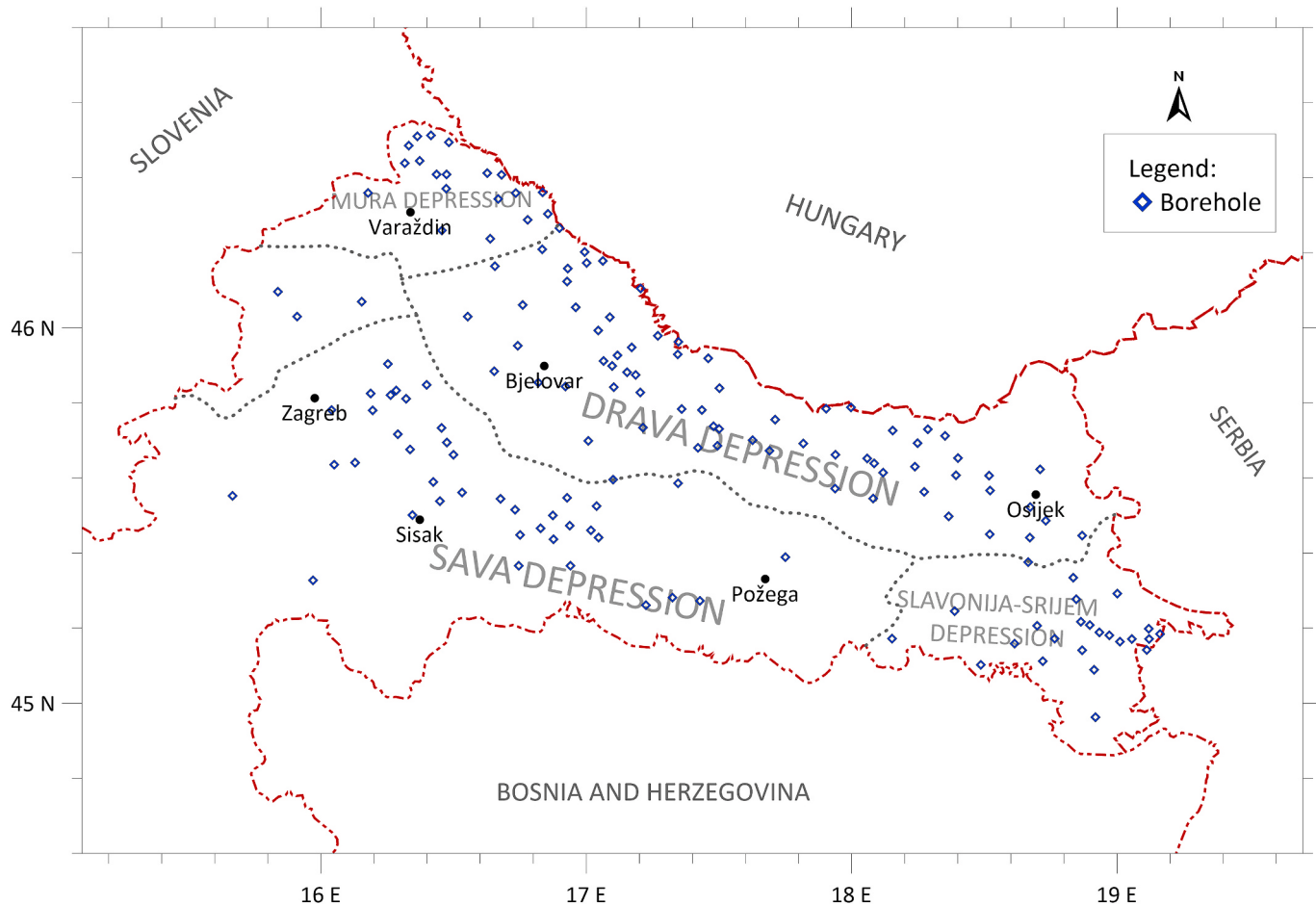


Fig. 2. Map of selected wells used in temperature analysis in the CPBS (depression borders according to Ref. [31]).

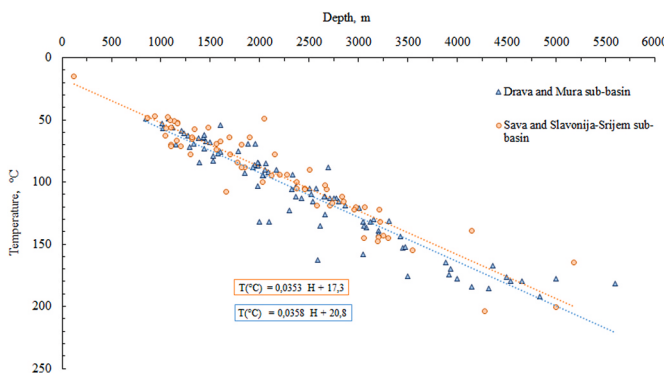


Fig. 3. Temperature data from selected 154 wells in the CPBS.

determining geothermal potential of an area [6]. Such maps indicate areas of higher interest and can dictate potential interest in further research and exploratory work to determine local and economical potential [7]. Kriging method used to interpolate between point data is often used in spatial analysis, e.g. in geology and petroleum engineering to determine trend of different subsurface properties such as porosity or permeability in regard to depth [8] or in survey to produce digital model of terrain [9]. The map of geothermal potential usually shows either geothermal gradient, e.g. Ref. [10], temperature values at a certain depth, e.g. cross section [11] or layout [12], or depth values of certain temperature values [13]. Along with geothermal gradient, heat flow maps are also derived and used to determine geothermal potential of the

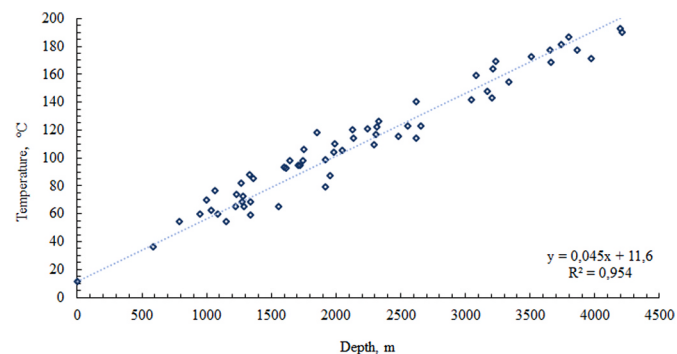


Fig. 4. Measured temperature data during the DST operation for selected wells in the CPBS.

area [14].

Therefore, the aim of this research is to construct a novel map of geothermal gradient and to compare the results with the previous study. Deliverables of this research will yield necessary input data during initial screening and exploration phase of the new geothermal sites. Furthermore, the geostatistical analysis used for interpolation is implemented and explained. During the next decade majority of the oil and gas wells in Croatia would need to be formally plugged and abandoned because of depletion of the existing reserves. To avoid these well assets being lost for good, their conversion to renewable source of energy is rather technically established and straightforward process, due to similarity of the production and collecting systems of petroleum and

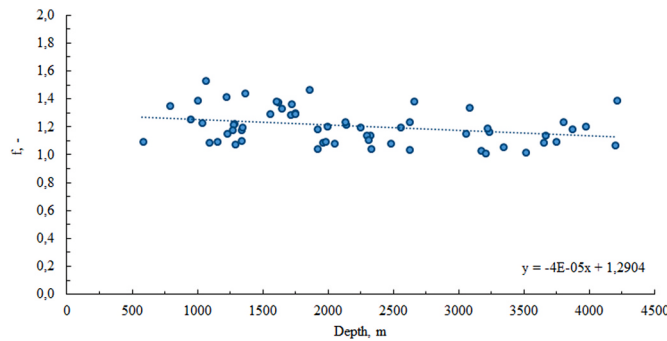


Fig. 5. Correction factor versus depth (for DST data).

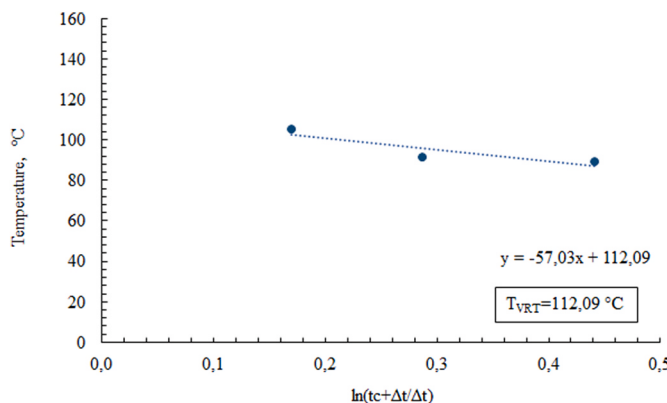


Fig. 6. Example of determining virgin rock temperature by using Horner method.

Table 1

Measured bottomhole temperatures with logged Δt and calculated t_c for an example well.

Data No.	Measured T_{BH} , °C	Δt , h	t_c , h	$\ln(t_c + \Delta t / \Delta t)$
1	88,9	6	3,3	0,442
2	91,1	10		0,287
3	105,0	18		0,170

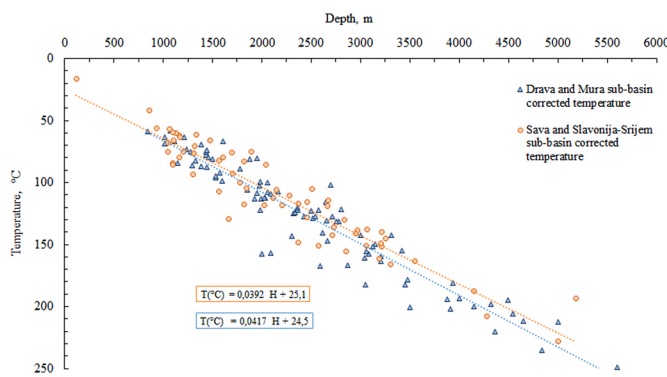


Fig. 7. Corrected temperature data from selected 154 wells in the CPBS.

geothermal industry. Existing wells in Croatia could be used either by directly producing geothermal fluid from discovered reservoirs [15], by enhanced geothermal systems (EGS) principle [16], by exceptional enhanced geothermal systems (EEGS) [17] or implementing method of closed-loop circulation via deep coaxial heat exchangers [18].

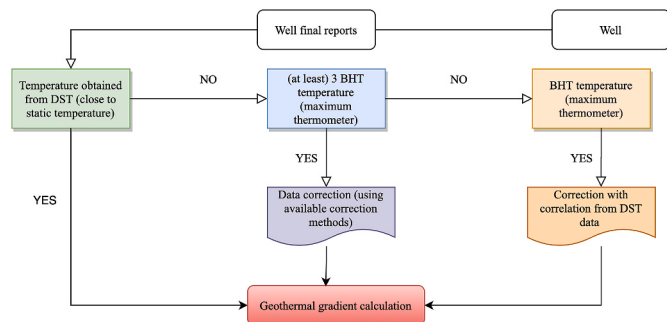


Fig. 8. Flow chart for geothermal gradient calculation.

Currently, there is a very favourable government stance towards geothermal energy. During the last few years, there were numerous tenders of exploration blocks announced for known brine reservoirs for possible private investing (Fig. 1). Most of the tendering process and documents preparation is carried out through Croatian Hydrocarbon Agency (www.azu.hr/en).

Since knowledge of geothermal gradient in certain area is of most importance when exploring geothermal reservoirs, and considering increased processes by government agencies to bring more geothermal sites into production, there was tremendous motivation to create completely new gradient map for northern part of the Croatia which would be solid foundation for all future researches in this area.

2. Methods

The geothermal gradient is a thermogeological parameter that describes the temperature change within the Earth's crust, which occurs due to the heat transfer process. The parameter is important when designing heating or power systems that utilize the underground as a heat source. The geothermal gradient is determined easily when two temperature values and their corresponding depths are known. The annual average surface temperature, T_s (°C), is usually used as a first value (with D_s (m) as first depth), while the other value should be the formation temperature T_f (°C) at a certain formation depth, D_f (m):

$$g_T = (T_f - T_s) / (D_f - D_s) \quad (1)$$

With the current technology it is not possible to directly measure the formation temperature at the static conditions [19], which is commonly referred as the undisturbed or virgin rock temperature (VRT). The temperature values, at greater depths, are commonly determined during the oil or gas well exploration works and drilling wildcat wells. There are several different methods of determining the formation temperature during this process. In most of the cases, the temperature values are measured with the maximum thermometer or with temperature logging tools [20]. With these methods, the temperature recorded is in fact temperature of mud during drilling operations. The temperature log continuously records the drilling mud temperature along a pre-determined length of a well. Serra [19] recommended that the logging should be run from the top of the well towards the bottom. This way, any disturbance of the drilling fluid caused by the wire line and the logging tool itself, can be avoided. Beside the temperature itself, this tool can be used to record differential temperature log, i.e. temperature gradient and depth, which can be used to determine thermal conductivity of formation [21]. Even though the temperature logs are a more precise method than maximum thermometer method, it is not standard procedure due to required time. The most common method is to measure maximum temperature of the drilling mud at the bottom of the well, with a maximum thermometer attached to different well log tools. Since maximum temperature measurements are usually performed relatively shortly after the cease of drilling operation and mud circulation, thermal equilibrium between the cooler drilling fluid and warmer formation is

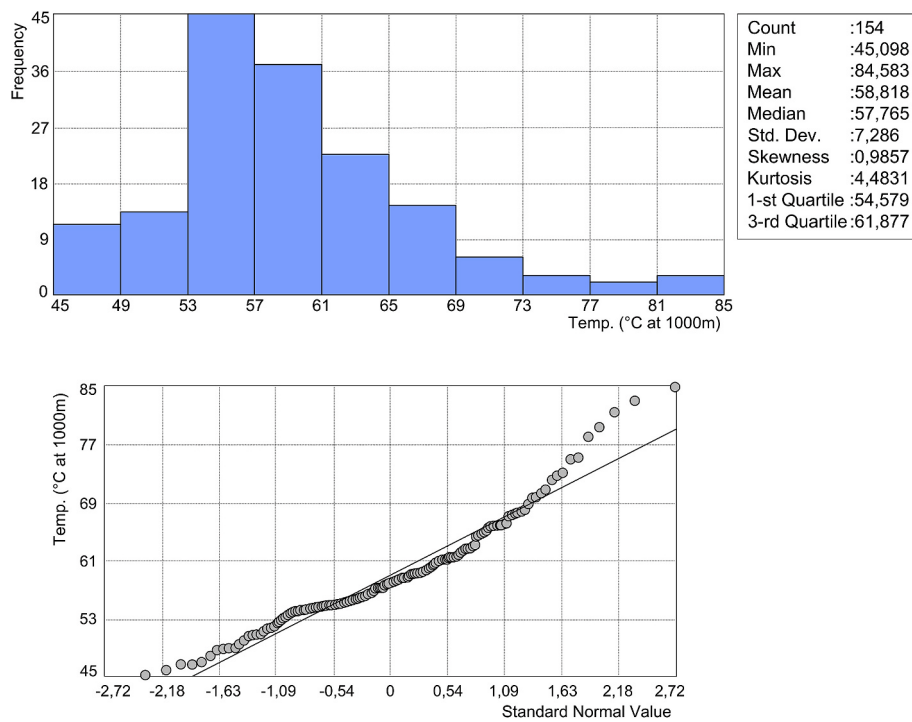


Fig. 9. Histogram and QQ diagram of data for 154 wells.

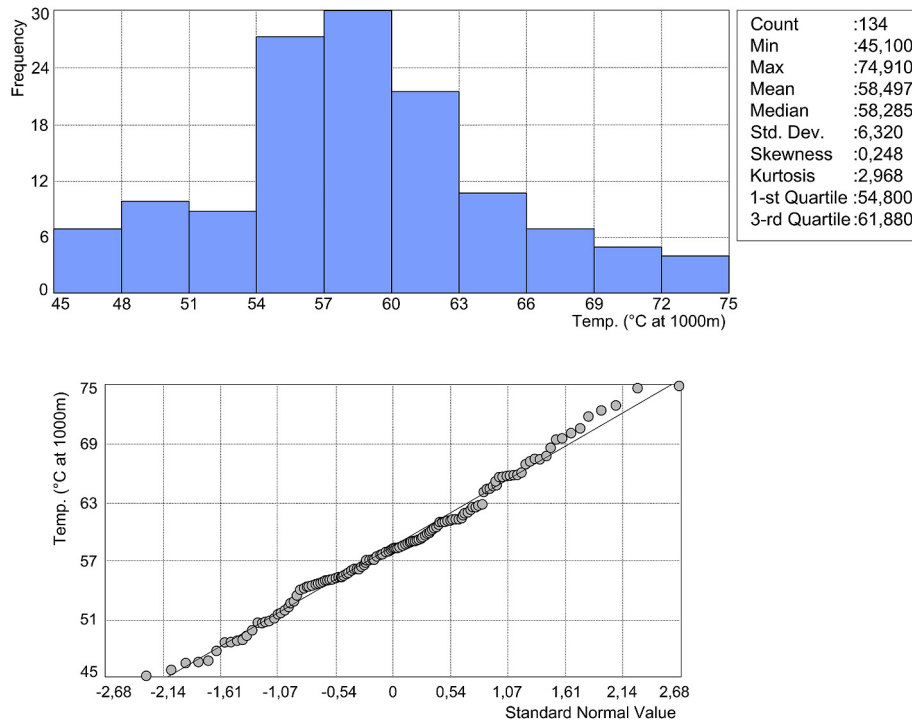


Fig. 10. Histogram and QQ diagram of data for 134 wells.

rarely achieved. Therefore, measured bottomhole temperature (BHT) is always lower than the initial static formation temperature. Nevertheless, the BHT data can be used to estimate the VRT. There are around 20 different methods of correcting the data, with most of them based on applied models of heat transfer in porous media. Hermanrud et al. [22] did extensive study on bias and error on 22 corrective methods of BHT, available at the time. The conclusion was that methods using two media model have the smallest deviation from the static values of formation

temperature.

2.1. Drill stem test

The determination of static formation temperature is of most importance to determine the geothermal gradient. Various researchers concluded that the temperature obtained from stabilized drillstem test (DST) can be taken as a value as close as possible to the VRT. The drill

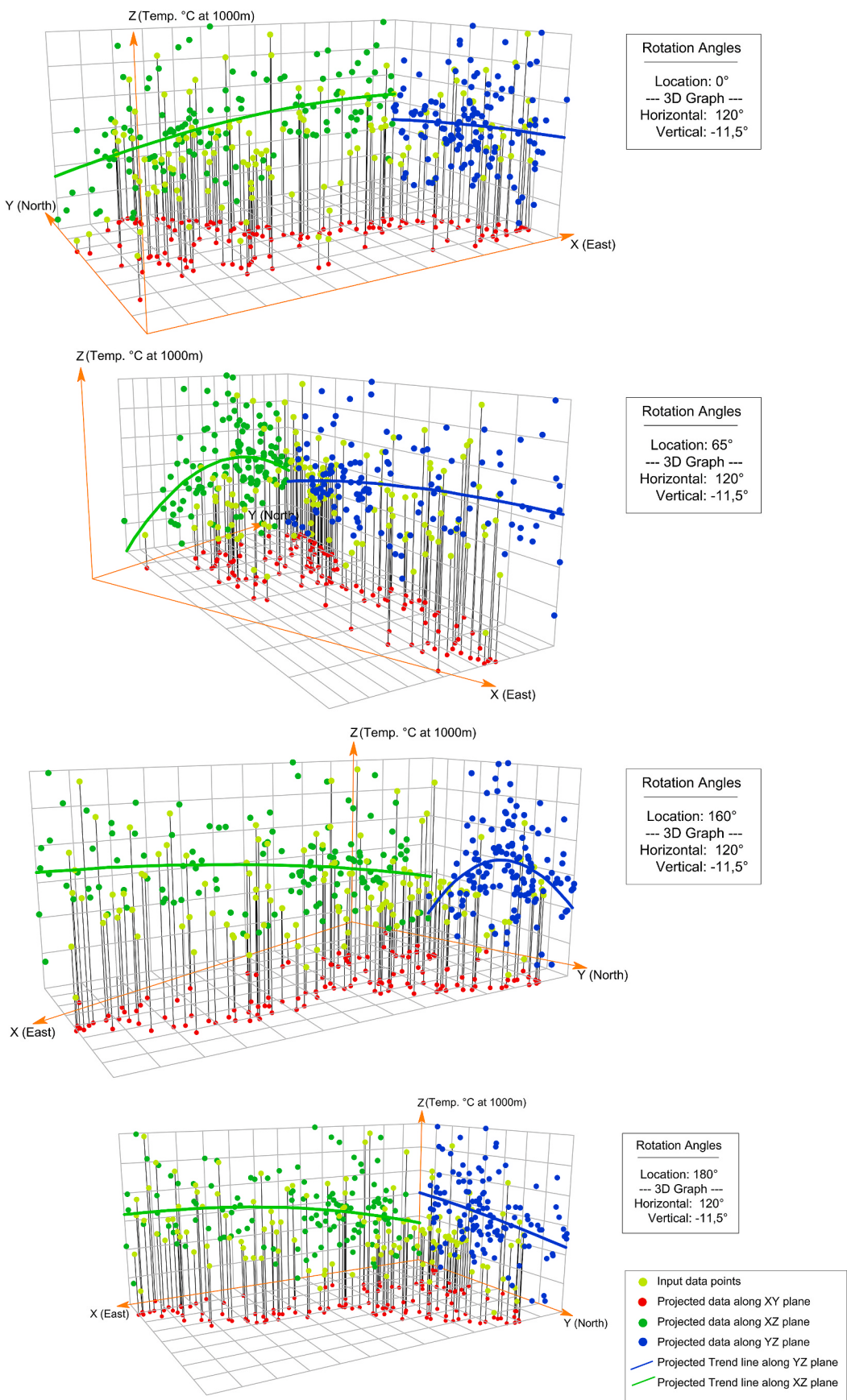


Fig. 11. Global trend curves at the rotation angle of 0°, 65°, 160° and 180°.

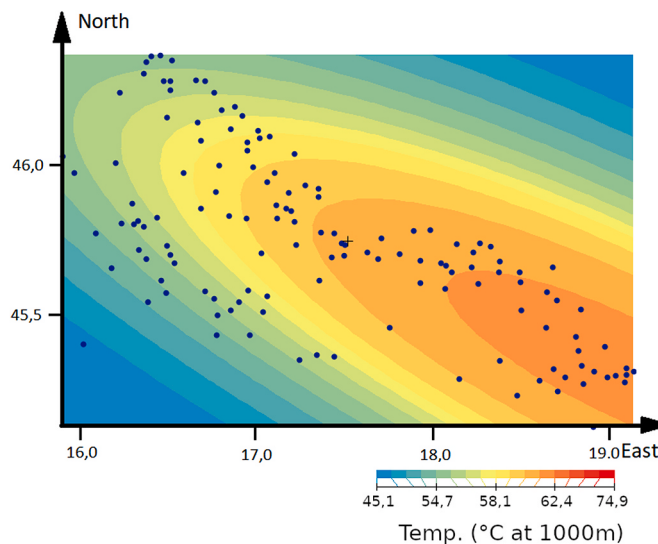


Fig. 12. Global trend model used for creating Kriging model.

stem test is a well-known method of well testing in petroleum engineering. The DST can be described as a temporary well completion which serves to sample the formation fluid and give early estimates of formation and fluid properties and give early estimation of commercial production of hydrocarbons. The tool for performing the DST isolates the zone of interest and allows the formation fluid to flow into the drill pipe or drillstem [23]. During the test, pressure and temperature are measured in sequence, with flow periods followed by shut-in periods. In petroleum engineering, pressure determined during the shut-in periods is significant since it can show formation characteristics, such as $k h$ product (permeability · formation thickness) and skin factor [23]. The temperature measured during this test is considered to be close to the VRT values [24]. This can be explained by the fact that during the fluid flow, the fluid being produced has its origin beyond immediate proximity to the wellbore wall. The zone near the wellbore wall is cooled down due to the circulation of colder drilling mud, while the thermal equilibrium of the formation in this area is disturbed. Special care has to be taken in cases when the DST experiences the so-called 'dry-runs' and in the case of significant gas inflow. The gas inflow will cause sub-cooling of the formation fluid due to the Joule-Thomson effect, resulting in lower recorded temperature.

2.2. Horner method

The most common method of correcting the bottomhole temperature due to logging with maximum thermometer is the Horner method. The method itself was derived from the same analogy of pressure build-up tests in petroleum industry. Both methods, the pressure build-up test and temperature evolution during the conductive heat transfer, have the same basis in Fourier's diffusivity equation. Lachenbruch and Brewer [25] were the first to use the Horner method for describing the temperature behaviour. The method takes three parameters into consideration: measured bottomhole temperature, T_{BH} ($^{\circ}\text{C}$); the circulation time of the drilling mud, t_c (i.e. time between the drilling being stopped and cessation of the circulation of the drilling mud (s)); time since the circulation stopped and the logging tool was set at the bottom of the well, Δt (s). Similar to the pressure build-up analysis, the measured BHT are related to the ratio of times Δt and t_c as:

$$T_{BH} = T_{VRT} + C \times \ln \left[\frac{\Delta t + t_c}{\Delta t} \right] \quad (2)$$

The method of determining the virgin rock temperature, T_{VRT} ($^{\circ}\text{C}$), is grapho-analytical. It comprises from charting the bottomhole

temperature values at the ordinate and corresponding values of natural logarithm of ratio $(\Delta t + t_c)/\Delta t$ on the abscissa. An intercept of an extrapolated straight line through measured temperature gives the value of the virgin rock temperature for the $(\Delta t + t_c)/\Delta t = 1$ [26]. The constant C represents the slope of the line, dependant on heat transfer rate and thermal conductivity of the formation:

$$C = \frac{q}{4\pi\lambda} \quad (3)$$

The bias and error study on different methods of correcting the BHT showed that the Horner's method mostly underestimate VRT values when compared to methods that use a few more parameters, usually rock properties [22]. How well the Horner's method will estimate the VRT depends on the accuracy of logging the BHT value, as well as accuracy in noting circulation time and time since the circulation stopped [24]. The biggest problem when inspecting the needed data, especially for old wells, is to determine the circulation time parameter, t_c (s). If the circulation time is not available, from well logs or drilling logs, it can be estimated as time needed for one or two complete cycles of circulating the fluid along the entire well. Bassiouni [21] determined that as long as the circulation time is estimated within reasonable limits, the influence of this parameter on overall result is minimal. Hermanrud et al. [22] conducted a study and determined an empirical correlation (based on personal experience of the authors) to calculate the t_c parameter:

$$t_c = \frac{1,3 + D}{1,3 - 0,091 \times D} \quad (4)$$

where D represents the depth of the well measured from the kelly bushing (km). Another common error when noting the BHT, comes when the wire of the logging tool disturbs the drilling fluid. This can cause convective disturbance in heat transfer that can result in recorded BHT being a few degrees different [19]. Usually, at least three recorded BHTs, at the same depth at different t_c , are required to have a good fit of the straight line.

Obviously, the most representative data and the ones that show true static temperature can be obtained in wells with long shut-in periods. However, this data is usually very scarce, due to the fact that measurements are rarely conducted in closed and abandoned wells. For this research, only few of such type of data was identified. Because of small number of such measurement and seeing how it would not have statistical impact on the results, the data was not included in the research.

2.3. Kriging method of interpolation

The geothermal map was calculated by using geostatistical Kriging method. Geostatistical modelling is a technique of creating a model of a surface by using various geostatistical methods. Using these methods detailed models are derived by using measured or known data regarding structural settings in order to evaluate characteristics of surfaces between observed data. These methods were first used in mining industry, where wellbores/boreholes are usually close-spaced, and later in oil&gas industry, geology etc. Statistical methods are based on the assumption that individual patterns are statistically independent of each other. This type of statistical independence is not applicable on spatial data describing areas rich in minerals, oil&gas or geothermal fluid. In order to describe various spatial dependence geostatistical methods were developed [27]. A variogram is a basic method of all geostatistical analysis, with which spatial dependence is valued. It is presented as an average squared difference of two values calculated as functions of distance between these two values [28]. The result of the variogram is an experimental variogram, which is approximated with a theoretical model and is an input value to the Kriging method.

With the Kriging method, it is possible to interpolate high-quality map data. The usual expression used to calculate values used for variogram is known as experimental semivariance [29]:

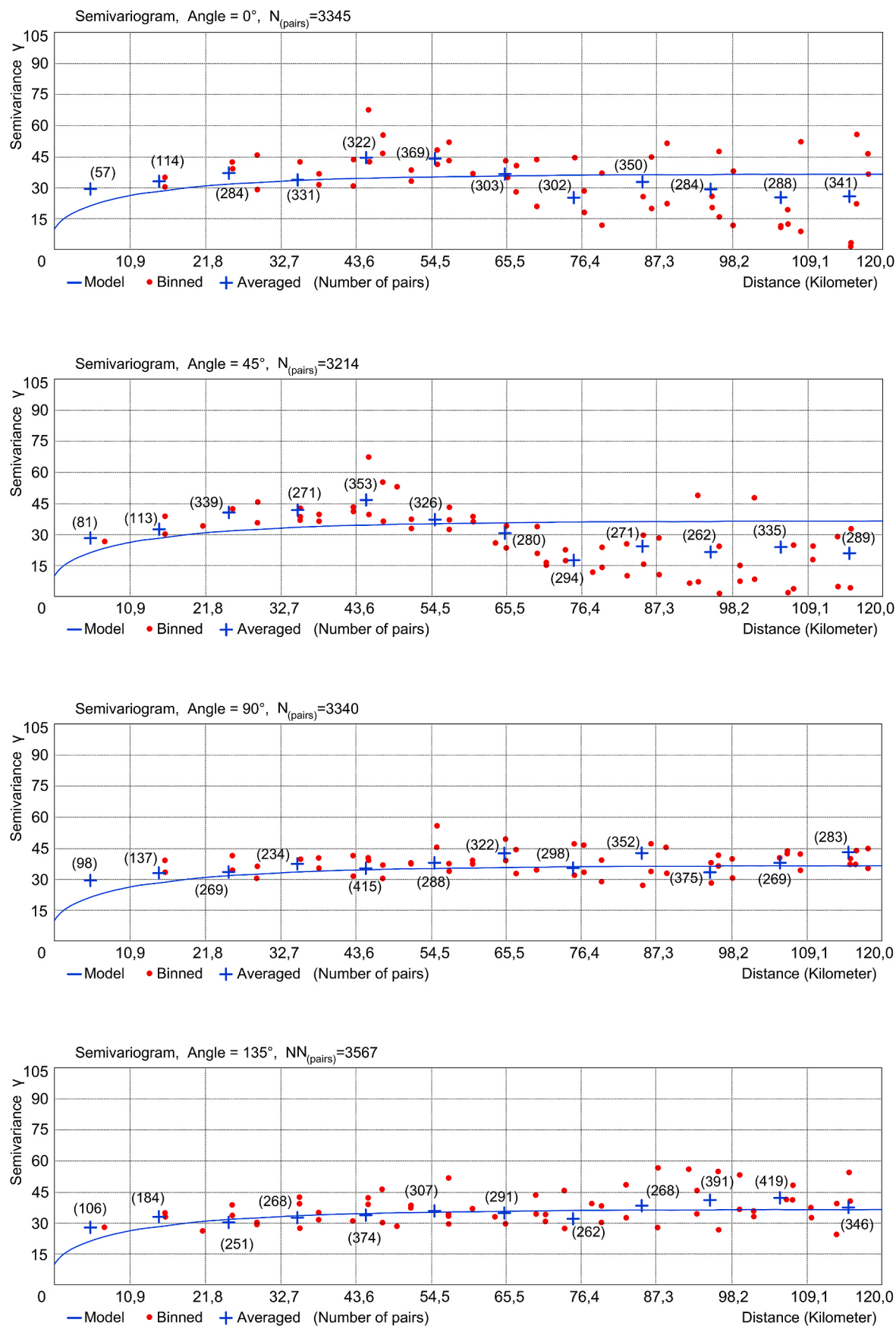


Fig. 13. Variograms in four different directions, at the rotation angle of 0°, 45°, 90° and 135°.

Table 2

Variogram parameters used for the interpolation.

Parameters of interpolation Kriging method			
Model	Ordinary	Partial sill	26
Semivariogram type	Spherical	Neighbours to include	5
Number of lags	12	Include at least	2
Lag size	10 000	Sector type	2
Range	52 000	Angle	0
Nugget	10	Search radius	52 000

$$\hat{\gamma}(h) = \frac{1}{2N(h)} \sum_{d_{ij}=h-\Delta/2}^{d_{ij}=h+\Delta/2} (z_i - z_j)^2 \quad (5)$$

where h is fixed distance or lag, d_{ij} is distance between i and j points, and Δ is spatial width with the centre located at h . Every pair of data value is considered, whose spatial distance falls within a spatial width. If a variogram can be modelled by using relatively simple equations, then the values for unknown locations can be evaluated by using the model which integrates weights needed for interpolation.

The Kriging method is a geostatistical method of determining most favourable linear estimation, with minimal variance. It can be used on points or on blocks [27]. It is a statistical method for estimation and interpolation method. By using Kriging method charts with standard

deviation can also be produced. Principal procedure of geostatistical interpolation, by using ordinary Kriging (OK), is based on determining values for points with no measurement in the grid, using ordinary linear weighted average for adjacent points with measurement, where optimal weight is defined with variogram model [30]. For a specific point:

$$z_p = \sum_{i=1}^n \lambda_i z_i \quad (6)$$

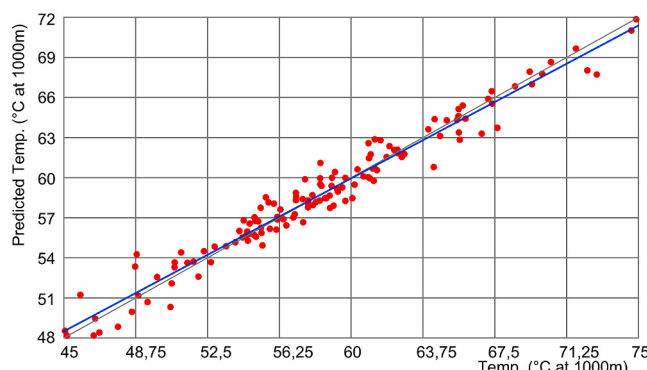
where λ_i is weighted coefficient for each location i , z_i control points (nearby known values), and z_p value estimated with Kriging. In the Kriging method weighted values can have positive as well as negative sign.

Table 3

Prediction errors on a set of 154 wells.

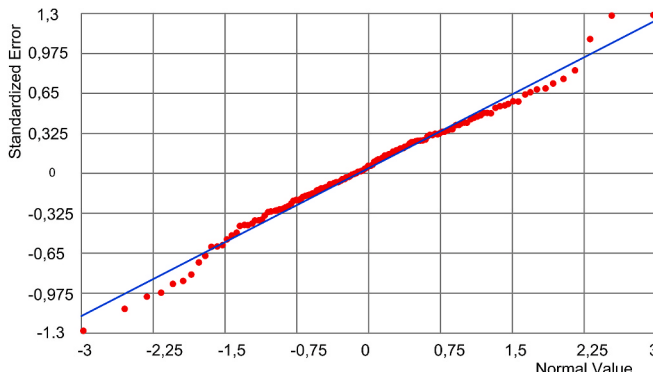
Prediction errors	
Mean	0,0322
RMS	2301
Average Standard Error	4096
Mean Standardized	0,008
RMS - standardized	0,766

Prediction 134 points

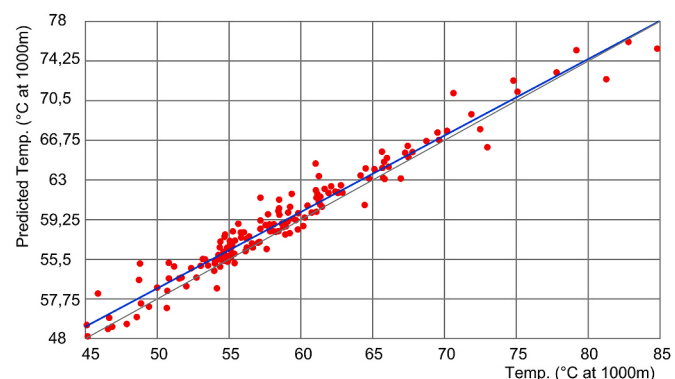


Regression function (Predicted):	$0,7391728*x + 15,2897989$
Prediction Errors	
Samples:	134 of 134
Mean:	0,0100871
Root-Mean-Square:	1,9011218
Mean Standardized:	0,0018981
Root-Mean-Square-Standardized:	0,7946177
Average Standard Error:	4,0874557

Normal QQPlot 134 points

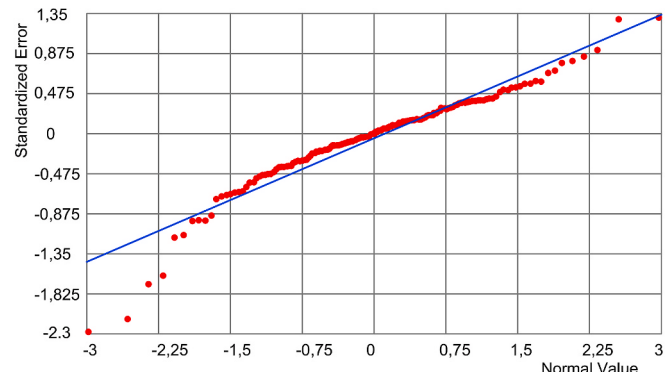


Prediction 154 points



Regression function (Predicted):	$0,7296227*x + 15,9130184$
Prediction Errors	
Samples:	154 of 154
Mean:	0,0321858
Root-Mean-Square:	2,3014434
Mean Standardized:	0,0078249
Root-Mean-Square-Standardized:	0,7661266
Average Standard Error:	4,0957969

Normal QQPlot 154 points

**Fig. 14.** Comparative comparison with a data set of 134 and 154 wells.

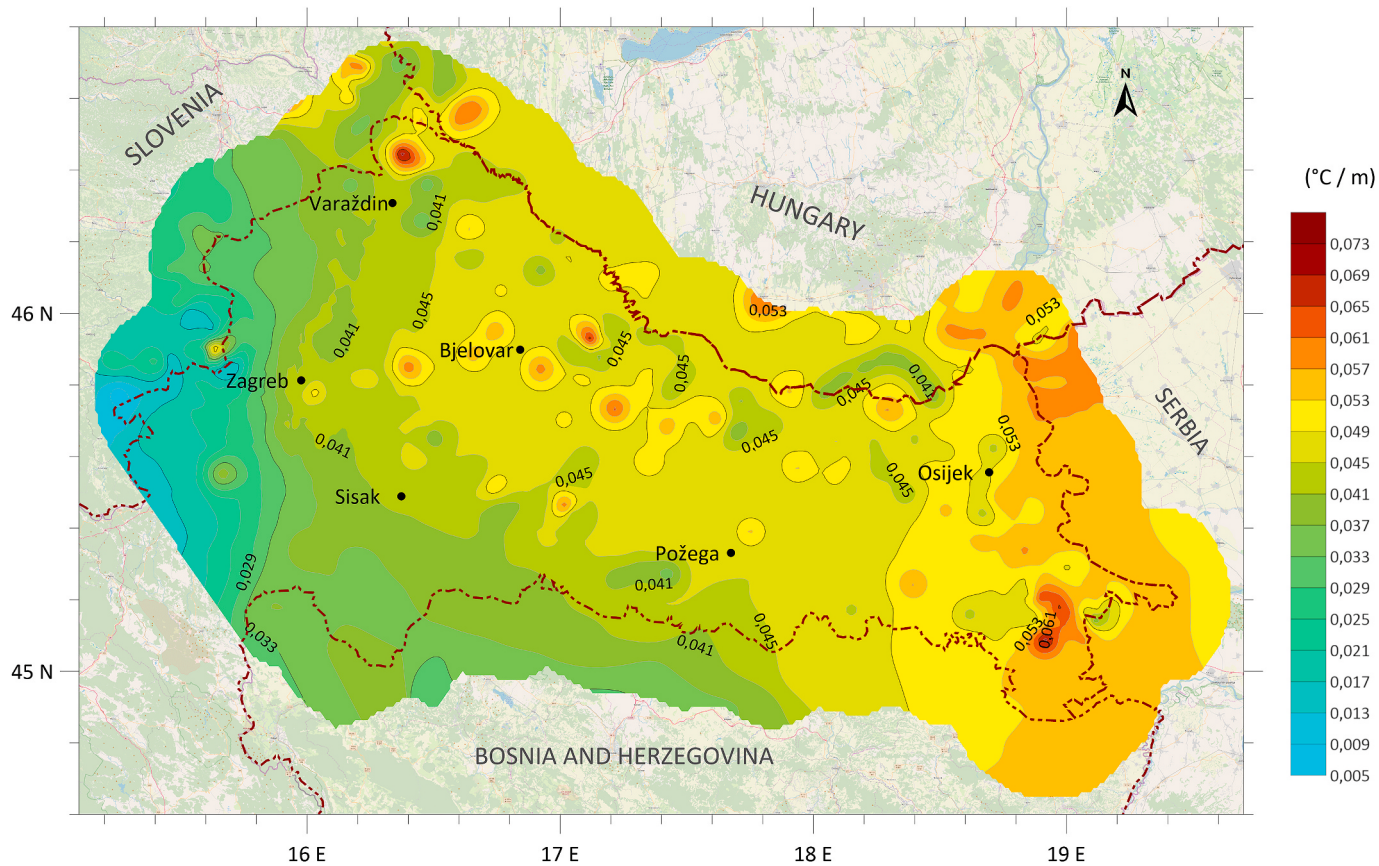


Fig. 15. Novel constructed map of geothermal gradient for the CPBS.

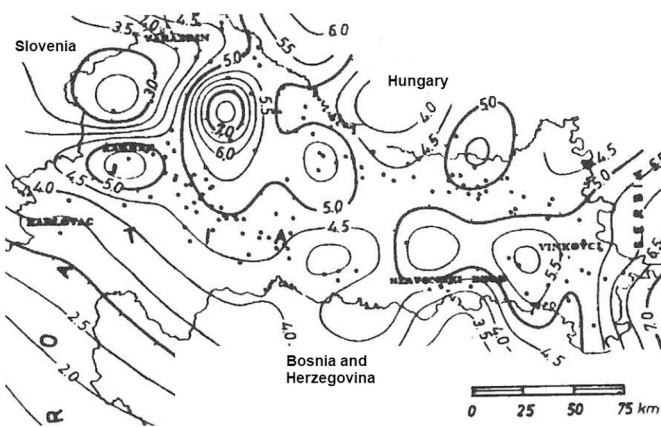


Fig. 16. Map of geothermal gradient in the area of the CPBS as previously constructed by Jelić et al. [5].

3. Calculation of geothermal gradient

The data on selected 154 wells, located in the CPBS (Fig. 2), regarding depth, temperature and location was collected from well logs (BHT data), DST logs, drilling logs and final reports regarding a certain well. All of the wells contained data for temperature measurement with maximum thermometer at the bottom of the well. Fig. 3 shows collected data of BHT in correlation with depth. The temperature data was divided into two main groups according to location, in relation to main subbasins (depressions), Sava - Slavonija-Srijem and Drava – Mura (Fig. 2).

Out of 154 wells, over 60 of them had available DST data. As mentioned, the temperature obtained during the DST operations, are

considered to be closest to the VRT as possible. With careful consideration when screening the DST data, some of the values were excluded due to 'dry-runs' or because of significant gas inflow. With this, out of 154 wells 61 of them had usable DST data. In cases when there was more than one good DST run, the values of depth and temperature were averaged, in order to have a single data for that well. The temperature data collected is seen on Fig. 4.

The geothermal gradient was calculated using equation (1), with average yearly surface temperature for the CPBS being determined at 11,6 °C [6]. These results were compared with the gradients obtained by using the bottomhole temperature for corresponding wells. The comparison was carried out as a ratio of the two corresponding values:

$$f = g_{T \text{ DST}} / g_{T \text{ BH}}$$

The said ratio represents dimensionless correction factors for the 61 data sets. The correction factors, f , versus depth are shown on Fig. 5. It is seen that a linear correlation between the correction factor and the depth can be established:

$$f = -0,00004 \cdot D + 1,2904$$

The same procedure was done for the data available for the Horner method. However, only 39 wells had good data to carry out the Horner correction of the BHT, with equations (2) and (4). Fig. 6 shows an example of grapho-analytical Horner method carried out on one selected well of 2325 m, with good data from BHT measurements (Table 1.). According to relation (2) it can be seen that the intercept on the ordinate gives value of the virgin rock temperature.

Out of the 39 wells, only 8 did not have DST data. The results of these 8 wells showed larger values of corrected temperatures, carried out with Horner's method, in comparison with a single BHT data. The corrected values were adopted as being representative temperature data for the 8 wells.

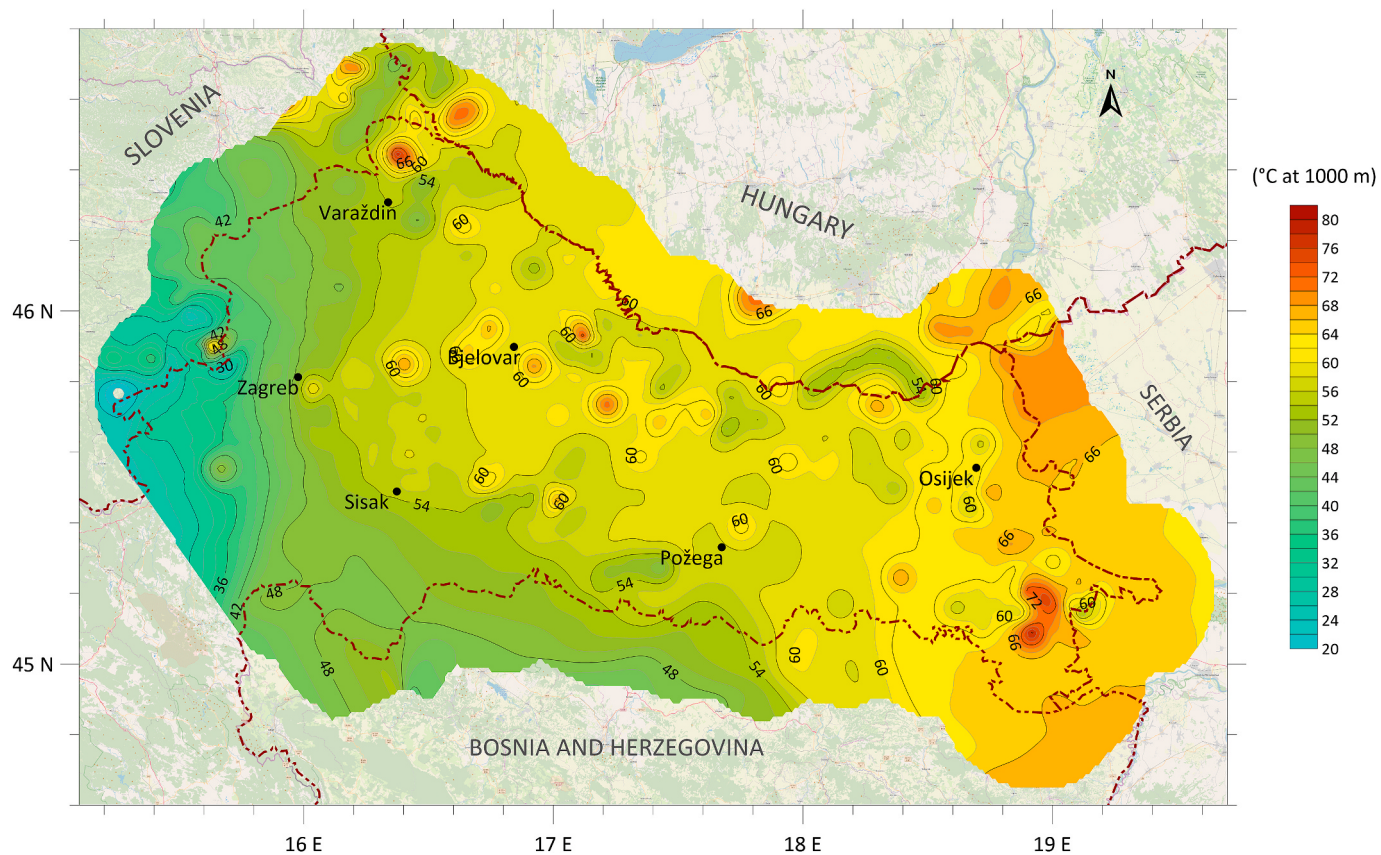


Fig. 17. Temperature at the depth of 1000 m in the CPBS.

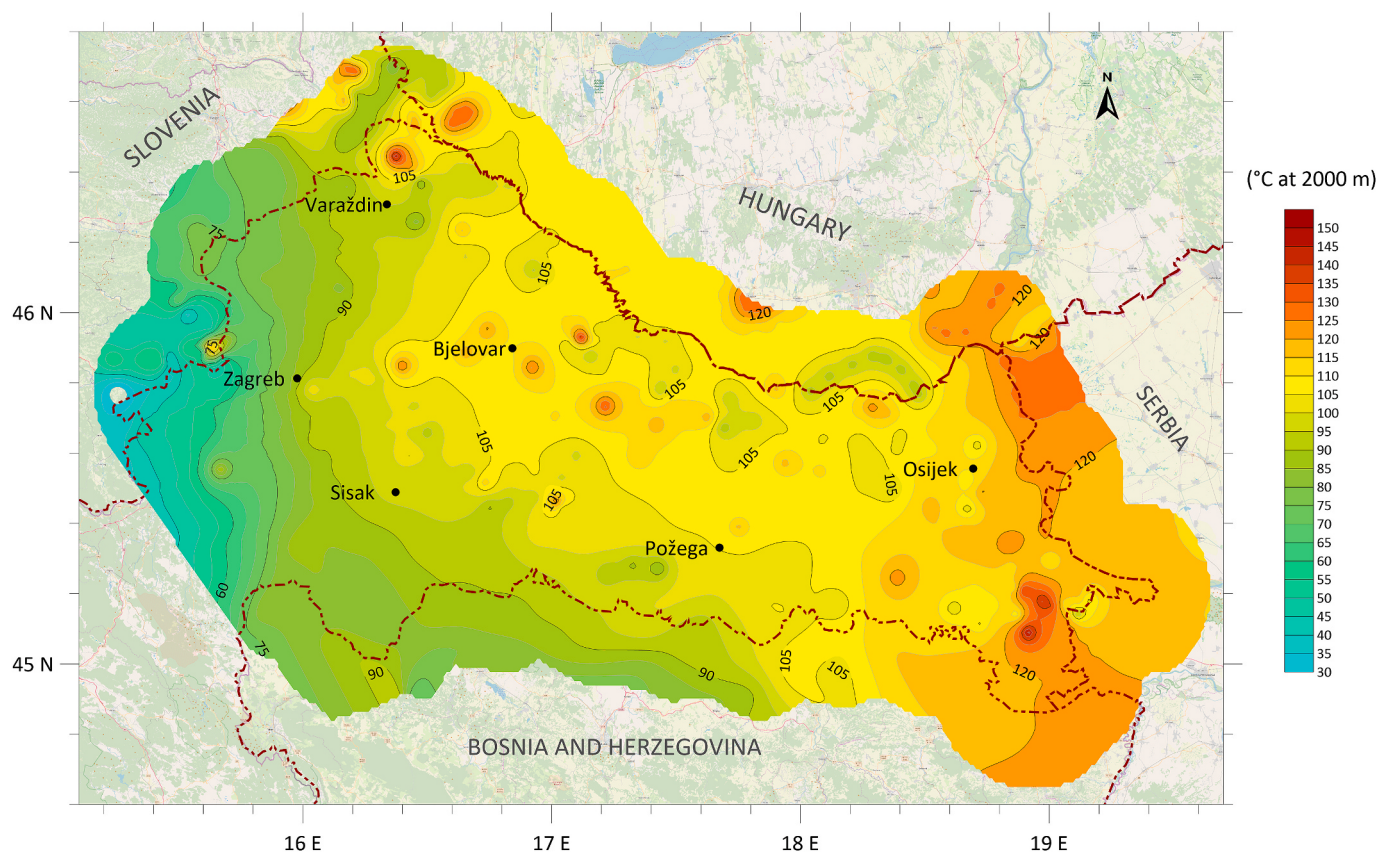


Fig. 18. Temperature at the depth of 2000 m in the CPBS.

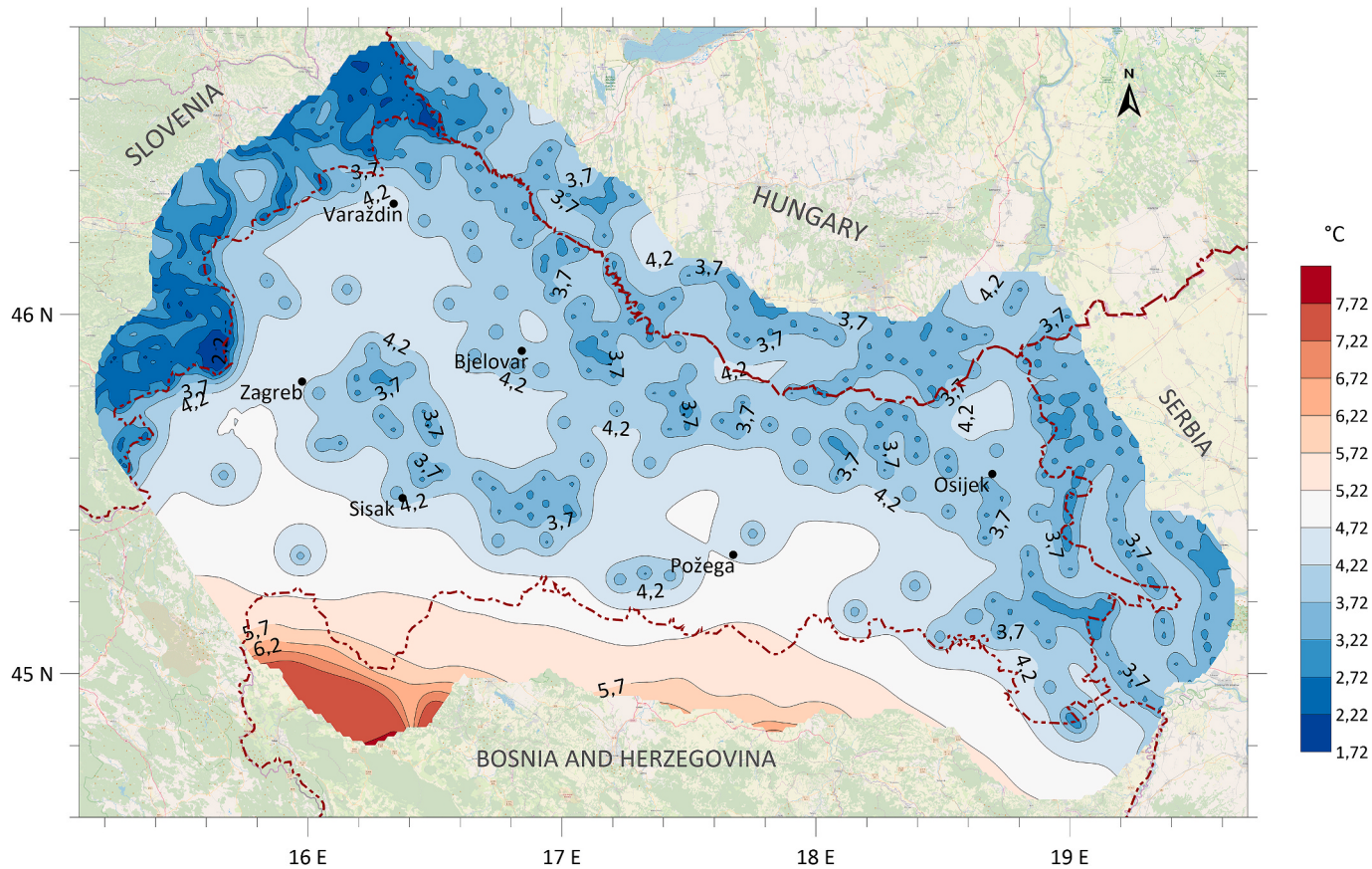


Fig. 19. Map of estimation standard deviation.

Out of 154 wells, 85 of them have only single bottomhole temperature value. Since the research showed that the temperatures obtained during the DST run show higher values than the temperatures obtained by using maximum thermometer, it was concluded that the BHT data for 85 wells can be corrected by using the factor determined by equation (6). For the remaining wells dimensionless factor f was calculated in regard to respective well depth, and the geothermal gradient calculated by data of BHT was corrected by the factor f . The resulting corrected temperature values are seen in Fig. 7.

The process of data collecting and calculation of geothermal gradient is shown by flow chart in Fig. 8.

4. General geological setting of the Croatian part of the Pannonian Basin system

Republic of Croatia can be divided into two main regions, the Pannonian Basin and Dinarides, from geological point of view. Out of these two regions the Pannonian Basin System is recognized with geothermal potential [5]. In general, the Pannonian Basin System is mostly lowland area, bordering with the Carpathian Mountains, Dinarides and Alps, comprising of igneous, metamorphic and sedimentary rocks, spanning from Precambrian to Quaternary age. The Croatian part of the Pannonian Basin System (CPBS) covers the area of around 30000 km² and was formed during the Neogene in three main megacycles [32]. The sediments of the 1st megacycle are of Lower Miocene and Middle Miocene age, and lithological very heterogeneous. They are mostly comprised of clastic sedimentary rocks, such as breccia, conglomerate, sandstone, claystone etc., and carbonates such as limestone and calcareous sandstone. The formations of 2nd megacycle are of Upper Miocene age, characterized with alterations of sandstones and marl. The 3rd megacycle formation are of Pliocene-Quaternary age, mostly comprised of beds of clays, sand, gravel and thin layers of lignite. The

Neogene sediments are overlying crystalline bedrock or Mesozoic sedimentary rocks, and underlying Quaternary deposits [33]. The oil and gas reservoirs are usually located within the sediments of 1st and 2nd megacycle [34]. The CPBS is usually divided into four main sub-basins Mura, Sava, Drava and Slavonija-Srijem, with variable Neogene and Quaternary sediment thickness. In Mura sub-basin sediment thickness reaches maximum of around 5000 m, as well as sediments in Sava sub-basin. Slavonija-Srijem sub-basin has the smallest sediment thickness, of around 4000 m, while in Drava sub-basin it can reach up to 7000 m [33]. Cvetković et al. [35] constructed new detailed pre-Neogene surface map, using published subsurface maps of the CPBS of different scale and level of detail. The compiled map shows depth to the base of the pre-Neogene surface with fault systems, depressions and structural highs.

5. Geostatistical analysis

Geostatistics assumes that naturally occurring phenomena are spatially dependencies [36]. In accordance with that theory, it is expected that the data taken within nearby proximity have more in common than the data from distant locations. In practice, it is not easy to sample the data, in a way that ideally covers the researched area. This is seen with the locations of the selected wells in this study since they are not distributed optimally within the research area. There are large areas where there no wells were drilled, and areas with the higher number of wells, due to oil and gas exploration and drilling (Fig. 2.). The aim is to obtain maps, using spatial interpolation, of geothermal gradient and temperatures at the depth of 1000 and 2000 m for the continental Croatia, based on data of 154 selected wells. Prediction model is explained using the data for temperatures at the depth of 1000 m.

The module Geostatistical Analyst, part of the ArcGIS software, was used for geostatistical analysis and interpolation [37]. The selected

geostatistical method is Kriging, first used in mining engineering in 1950 [38]. Neighbouring countries of Slovenia [39], Hungary [40] and Serbia [41] also used Ordinary Kriging for geostatistical interpolation of temperature data, in order to obtain temperature maps for each country. The temperature data from those maps were used in this analysis in order to enhance the extrapolation of data in the proximity of country borders. The data for Bosnia and Herzegovina could not be found in the literature, therefore on the southern border of continental Croatia, the extrapolation is of somewhat reduced accuracy.

The data for geostatistical Kriging interpolation must follow a normal distribution. The first testing of a normal distribution is to compare mean and median values. If these values are similar, it can be interpreted as a possibility of normality in the data. For an obtained set of data, this criterion is met since the mean value is 58,818 and the median value is 57,765 (Fig. 9). For further check of a normal distribution of data two ArcGIS tools were used, the histogram and QQ diagram (Normal Quantile-Quantile). Fig. 9 shows that the data have a small deviation towards the right side, which indicates that the higher values of temperature have a small deviation from normality. This is also indicated with QQ diagram.

In order to transform the data to have a normal distribution, logarithmic transformation was used. This did not produce results of good quality, therefore 15% of data with extreme values of temperature was separated. This ensured that the data had a normal distribution, as seen in Fig. 10.

The 13% of data (20 wells) are not disregarded since there is no indication that the data is corrupted. However, by using this data a good geostatistical model would be difficult to obtain. Therefore, the reduced set of data was used in order to create a variogram model for interpolation with normal distribution, as seen in Fig. 10. This model was applied for the entire set of data (for 154 wells) [42].

The global trend of data was verified, in order to determine data that conform to normal distribution. The trend shows that the normal distribution follows a parabolic curve, in the NE-SW direction. Maximum values are located in the middle of the parabolic curve, and minimum values at both ends of it. Fig. 11 shows data trends in relation to the local rotation of coordinate axes. For example, in the case of 0° rotation, it is seen that the trend is almost non-existed, while at the rotation of the data to 65° and 160° the trend is highly visible (see Fig. 12).

The global trend model is used to create a geostatistical model as a polynomial curve (Fig. 11.). This trend was removed before the calculation and selection of the variogram model and reversed at prediction [43].

By validating autocorrelation, using the semivariogram, it was determined that the spatial correlation is small and that is, by observing variogram models in every direction, similar (Fig. 13) [44]. It was concluded that the data can be classified as isotropic. Therefore, ordinary Kriging with a spherical model was used. The parameters for the variogram model are seen in Table 2.

Cross-validation was performed and compared on data from 134 to 154 wells (Fig. 14). The results show that the model is less reliable at extreme values when processing with all the data (154 wells). It is also seen that extreme values have the highest deviations, which has to be taken into account when interpreting the interpolated model.

The result obtained by cross-validation allows the assessment of whether the models and/or associated values are within acceptable limits. This means that if the mean prediction error is close to zero, the interpolated values will be close to the measured values. In case the interpolated values are closer to the measured values, the root-mean-square (RMS) prediction errors will have small values. The average RMS prediction errors are calculated as the square root of the average of the squared difference between measured values and interpolated values. If the RMS prediction error is lowest possible, then the model provides interpolated values of high accuracy. The values of the average standard error and the mean standardized prediction error should be lowest possible. Finally, the value of the RMS standardized prediction

error should tend to reach 1 [47]. Prediction errors on set of 154 wells are shown in Table 3.

The same model was used to interpolate values of geothermal gradient and temperatures at 2000 m.

6. Results and discussion

All of 154 geothermal gradients were used to construct the map of gradients in the area of the CPBS. In order to smooth out the geothermal gradient contour lines at the states borders, maps of temperature at 1000 m of depth or geothermal gradient, whichever was available, from neighbouring countries were taken into account. Beside the use of smoothing the contour lines at the border, data from these countries was used in order to confirm geothermal gradient values in the bordering area. A buffer zone extending approximately 50 km into neighbouring countries is seen on the map. For Slovenia data for temperatures at 1000 m [45] were used to calculate geothermal gradient, as well as Hungary's [46]. The Republic of Serbia had available data for the area of Vojvodina, which borders Croatia in the East, also for the temperature at 1000 m [41]. For Bosnia and Herzegovina there were no available data, to the best knowledge of authors. By using the geostatistic Kriging method, the data was interpolated, resulting in the final representation of the geothermal map, as seen on Fig. 15.

It can be seen form the map of geothermal gradient that the CPBS shows good potential when it comes to harnessing geothermal energy. This is especially evident in the areas where the geothermal gradient exceeds values 0,05 °C/m. When compared the previous map of Jelić et al. [5] (Fig. 16), it can be seen there is fairly good match, with values varying slightly in some areas. In the same study the reason for good gradients was attributed to the proximity of the Mohorovičić discontinuity, i.e. its relatively shallow position at around 30 km [4]. Geothermal anomalies present at few locations are attributed to convective heat flows and are already recognized as good potential in exploiting geothermal energy.

Based on the obtained geothermal gradients, temperature maps at a 1000 and 2000 m were also constructed and are seen on Fig. 17 and Fig. 18.

The map of temperatures at a depth of 1000 m is necessary for the initial screening process to determine potential of direct utilization of geothermal heat. From the map can be seen how deep wells must be constructed at certain area to directly utilize heat for example for central heating system, balneology, agriculture etc.

Since CPBS does not have saturated steam geothermal sources, only geopressured geothermal aquifers are available for electricity production. The map of temperatures at a depth of 2000 m is necessary for the initial screening process to determine how deep wells must be constructed for power production with Organic Rankine Cycle (ORC).

In Fig. 19 estimation standard deviation is shown for temperatures at 1000 m. It is seen that the highest deviation is in the southern part, towards country of Bosnia and Herzegovina, which is due to the lack of data in this area.

7. Conclusion

Since the new Renewable Energy Directive (EC 2018/2001) promotes the use of geothermal energy, the need was recognized to show potential via geothermal maps. Even though the previous research was extensive, the need arose to construct new maps, since the original digital representation is considered to be lost. The data from 154 wells was gathered and analysed. The analysis showed that there were 61 usable temperature records obtained during the drill stem test, which is considered to be a very close value to the static formation temperature, if the test is carried out properly. The records from 'dry-runs' and with gas inflow were discarded. 8 wells were identified as having good and reliable data to perform the Horner correction on the BHT data available. These values, of temperature obtained by DST and Horner

correction, were used to calculate the geothermal gradient. The remaining 85 wells had only single bottomhole temperature records. For those BHT data, a dimensionless factor, f , was determined. It represents the ratio of geothermal gradient calculated by using DST temperature and the one calculated with respective bottomhole temperature. It can be seen that this factor can be approximated with linear relation to depth. This linear relation was used to correct the remaining 85 BHT data.

With this data the new map of geothermal gradients was constructed, by using geostatistic Kriging method of interpolation. The same method was used for the map of temperatures at 1000 and 2000 m. By comparing the newly constructed maps with the previous research, it is seen that there is a fairly good match, which confirms good geothermal potential in the Croatian part of the Pannonian Basin System. The maps of temperatures at 1000 and 2000 m show areas of potential for utilizing geothermal resource for heating or power production respectively.

In future research map of geothermal gradient (or maps of temperature at a depth) can be used to analyse and select more feasible locations, especially with regard to heat demand. Since the use of geothermal energy for heating purposes is usually dependant on the distance between users and geothermal well, such analysis would show urban locations that could be among the first to prospect. Also, overlapping those favourable locations with the locations of abandoned wells (and the analysis of their respective available heating energy by using deep coaxial borehole heat exchangers) would show areas where feasible project could be developed first.

Declaration of competing interest

The authors declare that they have no known competing financial interests or personal relationships that could have appeared to influence the work reported in this paper.

Acknowledgments

The data permission was provided by the Croatian Ministry of Economy, Entrepreneurship and Crafts, as a part of 1st author doctoral study. The raw data was accessed in collaboration with the Croatian Geological Survey and Croatian Hydrocarbon Agency.

References

- [1] Directive (EU) 2018/2001 of the European Parliament and of the Council of 11 December 2018 on the promotion of the use of energy from renewable sources. Official Journal of the EU 2018;5:82–209. L 328/82.
- [2] INA Group Plc. Exploration and production. 2019. <https://www.ina.hr/about-ina/9845/core-business-9866/exploration-and-production-9867/9867>. [Accessed 3 December 2019].
- [3] Borović S, Marković I. Utilization and tourism valorisation of geothermal waters in Croatia. Renew Sustain Energy Rev 2015;44:52–63. <https://doi.org/10.1016/j.rser.2014.12.022>.
- [4] Maljković D, Guðmundsson JR, Živković S, Van Hemert R, Tumara D, Stupin K, Magnússon JR, Hjartarson H, Haizlip JR, Stöver MM. Geothermal energy utilisation potential in Croatia: Field and Study Visits' Report. Energy Institute Hrvće Požar 2016. <http://www.eihp.hr/wp-content/uploads/2017/07/Geothermal-Energy-Ut ilisation-Potential-in-Croatia-final-report.pdf>. [Accessed 28 April 2020].
- [5] Jelić K. Termičke osobine sedimentacionog kompleksa jugozapadnog dijela Panonskog bazena [dissertation]. Zagreb: University of Zagreb; 1979. Croatian.
- [6] Jelić K, Kevrić I, Krasić O. Temperaturi i toplinski tok u hrvatske. Proceedings of 1st Croatian Geological Congress, Opatija 1995:245–9. October 18–21.
- [7] Kehle RO, Schoeppe RJ, Deford RK. The AAPG geothermal survey of North America. Geothermics 1970;2:358–67.
- [8] Kis IM. Comparison of Ordinary and Universal Kriging interpolation techniques on a depth variable (a case of linear spatial trend), case study of the Sandrovac Field. Mining-Geol-Pet Eng Bull 2016;31(2):41–58. <https://doi.org/10.17794/rgn.2016.2.4>.
- [9] Medak D, Pribićević B, Krivoruchko K. Geostatistical analysis of bathymetric measurements: lake Kozjak case study. Geod List 2008;62(3):131–42.
- [10] Elbarbary S, Zaher MA, Mesbah H, El-Shahat A, Embaby A. Curie point depth, heat flow and geothermal gradient maps of Egypt deduced from aeromagnetic data. Renew Sustain Energy Rev 2018;91:620–9. <https://doi.org/10.1016/j.rser.2018.04.071>.
- [11] Jha SK, Puppala H. Assessment of subsurface temperature distribution from the gauged wells of Puga Valley, Ladakh. Geoth Energy 2017;5(1):3. <https://doi.org/10.1186/s40517-017-0061-4>.
- [12] Başel ED, Satman A, Serpen U. Predicted subsurface temperature distribution maps for Turkey. In: Proceedings of world geothermal congress. Bali; 2010. p. 1–7. April 25–29.
- [13] Toth AN. Creating a geothermal atlas of Hungary. Proceedings of 42nd Workshop on Geothermal Reservoir Engineering 2017;42(40.11):380–6. Stanford, February 13–15.
- [14] Aguirre G. Geothermal resource assessment: a case study of spatial variability and uncertainty analysis for the states of New York and Pennsylvania. Proceedings of Thirty-Eighth Workshop on Geothermal Reservoir Engineering 2013. Stanford, February 11–13.
- [15] Kurevija T, Vulin D. High enthalpy geothermal potential of the deep gas fields in Central Drava Basin, Croatia. Water Resour Manag 2011;25(12):3041–52. <https://doi.org/10.1007/s11269-011-9789-y>.
- [16] Caulk RA, Tomac I. Reuse of abandoned oil and gas wells for geothermal energy production. Renew Energy 2017;112:388–97. <https://doi.org/10.1016/j.renene.2017.05.042>.
- [17] Zhang L, Yuan J, Liang H, Li K. Energy from abandoned oil and gas reservoirs. In: Proceedings of SPE Asia pacific oil and gas conference and exhibition. Perth; 2008. October 20–22.
- [18] Macenić M, Kurevija T. Revitalization of abandoned oil and gas wells for a geothermal heat exploitation by means of closed circulation: case study of the deep dry well Pčelić-1. Interpretation 2018;6(1). <https://doi.org/10.1190/INT-2017-0079.1>. SB1–SB9.
- [19] Serra O. Fundamentals of Well-Log Interpretation (Vol 1): The Acquisition of Logging Data. Netherlands: Elsevier; 1984.
- [20] Bassiouni Z. Theory, measurement, and interpretation of well logs. Henry L. Doherty Memorial Fund of AIME, SPE; 1994.
- [21] Rider MH. The geological interpretation of well logs. Sutherland: Rider-French Consulting, Ltd.; 2000.
- [22] Hermanrud C, Cao S, Lerche I. Estimates of virgin rock temperature derived from BHT measurements: bias and error. Geophysics 1990;55(7):924–31.
- [23] Lee J. Well Testing. SPE: Richardson: Society of Petroleum Engineers of AIME; 1982.
- [24] Beardmore GR, Cull JP. Crustal heat flow: a guide to measurement and modelling. Cambridge University Press; 2001.
- [25] Lachenbruch AH, Brewer MC. Dissipation of the temperature effect of drilling a well in Arctic Alaska (No. 1083). US Government Printing Office; 1959.
- [26] Dowdle WL, Cobb WM. Static formation temperature from well logs—an empirical method. J Petrol Technol 1975;27(11):1–326.
- [27] Wellmer FW. Statistical evaluations in exploration for mineral deposits. Springer Science & Business Media; 2012.
- [28] Oliver MA, Webster RA. Tutorial guide to geostatistics: computing and modelling variograms and kriging. Catena 2014;113:56–69.
- [29] de Smith M, Goodchild M, Longley P. Geospatial analysis: A Comprehensive Guide to principles, Techniques and Software Tools. third ed. Leicester: SPLINT; 2009.
- [30] Negreiros J, Painho M, Aguilar F, Aguilar M. Geographical information systems principles of ordinary kriging interpolator. J Appl Sci 2010 Jan 1;10(11):852–67.
- [31] Malvić T. Regional turbidites and turbiditic environments developed during Neogene and Quaternary in Croatia. Materials and Geoenvironment 2016;63(1):39–54.
- [32] Velić J, Weisser M, Saftić B, Vrbanac B, Ivković Ž. Petroleum-geological characteristics and exploration level of the three Neogene depositional megacycles in the Croatian part of the Pannonian Basin. Nafta 2002;55:11–23.
- [33] Saftić B, Velić J, Szántó O O, Juhász G G, Ivković Ž. Tertiary subsurface facies, source rocks and hydrocarbon reservoirs in the SW part of the Pannonian Basin (Northern Croatia and South-Western Hungary). Geol Croat 2003;56:101–22.
- [34] Velić J, Malvić T, Cvetković M, Vrbanac B. Reservoir geology, hydrocarbon reserves and production in the Croatian part of the Pannonian Basin System. Geol Croat 2012;65:91–101. <https://doi.org/10.4154/gc>.
- [35] Cvetković M, Matos B, Rukavina D, Kolenović Mocilac I, Saftić B, Baketarić T, Baketarić M, Vujić I, Stopar A, Jarić A, Paškov T. Geoenergy potential of the Croatian part of Pannonian Basin: insights from the reconstruction of the pre-Neogene basement unconformity. J Maps 2019;15(2):651–61. <https://doi.org/10.1080/17445647.2019.1645052>.
- [36] Miller HJ. Tobler's first law and spatial analysis. Ann Assoc Am Geogr 2004;94(2):284–9.
- [37] Johnston K, Ver Hoef JM, Krivoruchko K, Lucas N, Magri A. ArcGIS 9: ArcGIS Geostatistical Analyst Tutorial. United States of America: ESRI; 2008.
- [38] Chang KT. Introduction to geographic information systems. Boston: McGraw-Hill Higher Education; 2006. p. 117–22.
- [39] Rajver D, Ravnik D. Geothermal pattern of Slovenia-enlarged data base and improved geothermal maps. Geologija 2002;45(2):519–24.
- [40] Goetzl G, Zekiri F, Lenkey L, Rajver D, Svasta J. Summary Report: Geothermal models at supraregional scale, Report of TRANSENRGY project. 2012. <http://transenergy-eu.geologie.ac.at/results>. [Accessed 8 May 2020].
- [41] Geothermal Atlas of Vojvodina. 2010. http://www.psemr.vojvodina.gov.rs/images/Studije/Geotermalna-energija/Geotermalni_atlas_AP_Vojvodine.pdf. [Accessed 25 November 2019].
- [42] Krivoruchko K. Spatial statistical data analysis for GIS users. Redlands: Esri Press; 2011.
- [43] Berke O. Modified median polish kriging and its application to the Wolfcamp-Aquifer data. Environmetrics: The official journal of the International Environmetrics Society 2001;12(8):731–48.

- [44] Chiles JP, Delfiner P. Geostatistics: modeling spatial uncertainty. New York: John Wiley & Sons; 2009.
- [45] EGIP GeoZS Geothermal Map. https://biotit.geo-zs.si/gis/rest/services/EGIP/EGIP_geothermal_map/MapServer. [Accessed 25 November 2019].
- [46] Schellschmidt R, Hurter S, Förster A, Huenges E. Atlas of geothermal resources in Europe. Brussels: Office for Official Publications of the European Communities; 2002.
- [47] Ali HZ. Cross-validation of elevation data interpolation, vol. 32. Al-Rafidain University College For Sciences; 2013. p. 109–19.